

# Adaptive Time Reversal Beamforming in Dense Multipath Communication Networks

Yuanwei Jin  
Engineering and Aviation Sciences  
University of Maryland Eastern Shore  
Princess Anne, MD 21853

José M.F. Moura and Nicholas O'Donoghue  
Electrical and Computer Engineering  
Carnegie Mellon University  
Pittsburgh, PA 15213 \*

## Abstract

*In this paper, we study the transmit time reversal beamforming in rich scattering environments in a multi-user wideband communication network. We consider the downlink time reversal transmission where a base station communicates with many users. The base station has multiple antennas and the user has a single antenna. Due to the presence of scatterers, conventional transmit beamforming interferes (crosstalk) with nearby users. We design a wideband beamformer that focuses on the intended user while minimizing its interference to other users. We calculate the sum rate capacity of the proposed time reversal transmission scheme. We also show that the proposed beamformer is equivalent to time reversal focusing and nulling and yields better performance than the conventional delay line wideband beamformer. We verify our results using realistic scattering channels simulated by finite-difference time-domain modeling of the scattering environment.*

## 1 Introduction

The physical characteristics of the channel between the transmit and receive antennas affect many aspects of the design of a wireless communication system. In a rich scattering environment, multipath propagation is very common. This paper is concerned with showing that exploiting rich scattering present in the environment enables system performance improvement over many existing processing techniques. Time reversal is a technique that utilizes rich scattering environment to achieve higher resolution and detectability. Our prior work [1, 2], as well as work of others, has shown that using time reversal in a communication system provides us less complexity of equalizer, low intersymbol interference (ISI), and high communication security [3]. In this paper, we develop a time reversal beamformer to enhance system capacity in the downlink transmission.

We consider a wireless communication scenario where a base station simultaneously communicates with several

users. To reduce the crosstalk between these users, the available bandwidth is partitioned into several independent channels. Common approaches include frequency division multiple access (FDMA), time division multiple access (TDMA), and code division multiple access (CDMA). Transmit beamforming is a downlink transmission strategy that enables signal separation by directing one or multiple beams simultaneously towards users at different spatial locations. This type of multiuser communication scheme is called Space Division Multiple Access (SDMA) [4, 5, 6]. The key idea in SDMA is to enable the base station with multiple antennas to send/receive multiple data streams to/from different users on the same time-frequency channels while separating them in the spatial domain.

However, transmit beamforming is difficult in a dense scattering environment, for example, metropolitan areas or indoor office buildings. Due to the presence of scatterers, the array, by directing a beam towards a user station, causes crosstalk interference to nearby users. Furthermore, the array can not separate signals sent to two users at the same azimuth even though these two users may be at a very different down range location. Unless the base station array can account for all of the scatterers in the environment, unwanted crosstalk is inevitable. The need for high data rate wireless communication in challenging multipath rich conditions has motivated extensive research and development of multi-antenna systems.

In this paper, we apply time reversal to the multi-antenna downlink wideband broadcast channels in dense multipath. Each base station has multiple antennas, while each user has a single antenna. By time reversal, an antenna array can focus on or null out, temporally and spatially, wideband signals on the intended user locations. Both focusing and nulling schemes have been experimentally demonstrated in the electromagnetic domain [7].

Time reversal relies on the fact that the transmitter “knows” the channel into which it is transmitting, which requires a feedback mechanism. This is generally true for Time Division Duplex (TDD) networks such as is proposed for the IEEE 802.16 (WiMax) networks. However it is also possible in a Frequency Division Duplex (FDD) network for

\*This joint work is funded by the Defence Advanced Research Projects Agency through the Army Research Office under grant no. W911NF-04-1-0031

a transmitter to have Channel State Information (CSI), provided sufficient feedback exists. For example, we can use time reversal on a 1xEVDO network. 1xEVDO (which is an FDD network) has the distinct advantage in that it has Time Division Multiplexing (TDM) air interface on the forward link. This means that the base station is free to transmit a non-standard waveform (the time reversed channel response in this case) within a time slot without interfering with other mobiles. To implement time reversal, the user terminal must provide feedback to the base station. Let us consider a user terminal that can estimate the forward link channel from the base station to the user. The user terminal then feeds the CSI back to the base station on one of the feedback channels. On reception of the CSI, the base station forms a wideband beamformer to transmit time-reversed signals to focus on the intended user while suppressing the interference from other users.

The contributions of this paper are as follows. We design a time reversal beamformer (TRBF) that utilizes the rich scattering to focus on intended targets while minimizing the information leakage to unintended users. We show that the proposed beamformer is equivalent to time reversal focusing and nulling. Time reversal focusing improves the signal-to-noise ratio at the intended users, while nulling reduces the crosstalk among user streams. We also derive the sum data rate capacity of the proposed TRBF. We show that a rich scattering environment improves system capacity. TRBF contrasts with a coding scheme called dirty paper coding (DPC) [8]. DPC is a multi-user encoding strategy based on interference pre-subtraction. DPC can achieve maximum capacity in MIMO broadcast channels, but is difficult to implement in practical systems due to its high computational burden [9, 10], while TRBF has relatively easy implementation. Finally, we use finite-difference time-domain electromagnetic dynamic simulations to demonstrate the effectiveness of the proposed broadband beamforming scheme in a dense multipath environment.

## 2 Time Reversal Space-Time Focusing

In this section, we discuss space-time focusing by time reversal. Fig. 1 depicts the downlink beamformer scenario where a base station communicates with users denoted by  $m$  and  $k$ . The base station has  $N$  antennas, each is connected with a filter. Let  $G(\omega; \mathbf{r}_n, \mathbf{x})$  denote the  $n$ -th filter transfer function of the  $n$ -th antenna located at  $\mathbf{r}_n$  to be focused on the intended user at location  $\mathbf{x}$ . This implies that the filter transfer function is space-frequency dependent in a rich scattering environment. Let

$$\mathbf{g}(\omega) = [G(\omega; \mathbf{r}_1, \mathbf{x}), G(\omega; \mathbf{r}_2, \mathbf{x}), \dots, G(\omega; \mathbf{r}_N, \mathbf{x})]^T \quad (1)$$

be the collection of filter space-frequency responses. The vector  $\mathbf{g}(\omega)$  can be considered as a generalized beamforming weight vector. Similarly, let  $C(\omega; \mathbf{x}_m, \mathbf{r}_n)$  denote the

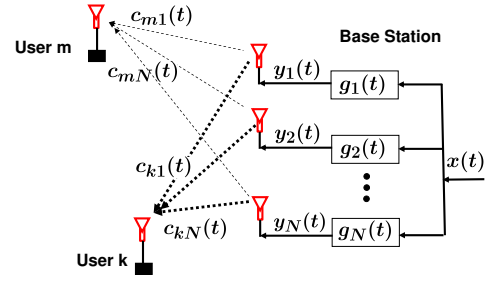


**Figure 1. Time reversal beamformer. Filters  $g_n(t)$  are designed to communicate with user  $m$  and user  $k$  simultaneously.**

channel transfer function between the  $m$ -th user at location  $\mathbf{x}_m$  and the  $n$ -th antenna of the base station at location  $\mathbf{r}_n$ , and let

$$\mathbf{c}_m(\omega) = [C(\omega; \mathbf{x}_m, \mathbf{r}_1), C(\omega; \mathbf{x}_m, \mathbf{r}_2), \dots, C(\omega; \mathbf{x}_m, \mathbf{r}_N)]^T$$

be the collection of channel space-frequency response vector. The general focusing spot can be written as

$$f(\mathbf{x}) = \int \sum_{n=1}^N G(\omega; \mathbf{r}_n, \mathbf{x}) C(\omega; \mathbf{x}_m, \mathbf{r}_n) d\omega \quad (2)$$

$$= \int \mathbf{g}^T(\omega, \mathbf{x}) \mathbf{c}(\omega, \mathbf{x}_m) d\omega. \quad (3)$$

Time reversal experiments, in acoustics and in electromagnetic [7], have proven that space-time focusing occurs in a rich multipath environment if the following condition is satisfied:

$$G(\omega; \mathbf{r}_n, \mathbf{x})|_{\mathbf{x}=\mathbf{x}_m} = C^*(\omega; \mathbf{x}_m, \mathbf{r}_n). \quad (4)$$

Under this condition, we have

$$f(\mathbf{x})|_{\mathbf{x}=\mathbf{x}_m} = \int \|\mathbf{c}(\omega, \mathbf{x}_m)\|^2 d\omega. \quad (5)$$

Studies in time reversal have shown that time reversal is effective in a point-to-point communication link in a multipath rich environment. In the presence of multiple users, our interest is in reducing the interference to other users while focusing on the intended users. Thus the main goal is focusing and anti-focusing in the space-time domain.

Time reversal focusing is influenced by two factors: signal bandwidth and correlation distance [11]. For two users separated by a correlation distance, their channel responses are approximately orthogonal, which yields maximum capacity. The correlation distance can be defined as:

$$D(\delta\mathbf{r}) = \frac{\int G(\omega; \mathbf{r}, \mathbf{x}) G^*(\omega; \mathbf{r} + \delta\mathbf{r}, \mathbf{x}) d\omega}{\int |G(\omega; \mathbf{r}, \mathbf{x})|^2 d\omega}. \quad (6)$$

Plotting the correlation distance as a function of  $\delta\mathbf{r}$  shows that this value peaks at  $\delta\mathbf{r} = 0$  and decreases as  $\delta\mathbf{r}$  increases. The 3-dB width indicates the spatial resolution of the focusing effect by time reversal. This resolution generalizes the beamwidth of the conventional narrowband beamformer, where  $\delta\mathbf{r}$  becomes the azimuth angle.

### 3 Multi-user Time Reversal Beamforming

#### 3.1 Time Reversal Beamformer Design

Next, we design the beamformer  $\mathbf{g}(\omega)$  for a base station to focus on the intended user  $m$  while suppressing the crosstalk (interference) among users. We let

$$\mathbf{H}(\omega) = \begin{bmatrix} \mathbf{c}_1^T(\omega) \\ \vdots \\ \mathbf{c}_M^T(\omega) \end{bmatrix} \quad (7)$$

be the channel matrix between the base station antennas and  $M$  users, and

$$\mathbf{i}(\omega) = \mathbf{H}(\omega)\mathbf{g}(\omega) \quad (8)$$

be the overall response of all the users. The time reversal beamformer at  $\omega$  minimizes the total signal power for all the users

$$\mathbf{g}(\omega) = \arg \min_{\mathbf{g}(\omega)} \int \|\mathbf{i}(\omega)\|^2 d\omega \quad (9)$$

subject to the following focusing constraint

$$\int \mathbf{g}^T(\omega)\mathbf{c}_{m,n}(\omega)d\omega = \gamma_m, \quad (10)$$

where  $\gamma_m$  is the focusing gain for user  $m$  and will be determined by the channel and the constraint on total transmit power. Using the Lagrange multiplies and the functional derivative of complex variables [12], we can solve for  $\mathbf{g}(\omega)$ :

$$\mathbf{g}(\omega) = \eta_m [\mathbf{H}^H(\omega)\mathbf{H}(\omega)]^{-1} \mathbf{c}_m^*(\omega) \quad (11)$$

where

$$\eta_m = \frac{\gamma_m}{\int \mathbf{c}_m^T(\omega)(\mathbf{H}^H(\omega)\mathbf{H}(\omega))^{-1} \mathbf{c}_m^*(\omega)d\omega}. \quad (12)$$

Here we assume that the matrix  $\mathbf{H}^H(\omega)\mathbf{H}(\omega)$  is invertible. In general, this inversion can be computed by singular value decomposition. The phase conjugate appearing in Eqn. (11) indicates that the resulting filter  $\mathbf{g}(\omega)$  for user  $m$  is a time-reversal replica of  $\mathbf{c}_m(\omega)$ . The filter can also be considered as a generalized minimum variance distortionless response (MVDR) filter at frequency  $\omega$ . The time domain filter  $g_n(t)$  can be designed by converting the frequency response of (11) into the time domain by inverse Fourier transform.

#### 3.2 System Model and Sum Rate Capacity

The sum rate capacity refers to the aggregate data rate of all the users in a network. Given (11), we introduce the system model illustrated in Fig.1.

Let  $\mathbf{G}(\omega)$  denote the collection of beamformers

$$\mathbf{G}(\omega) = [\mathbf{g}_1(\omega), \dots, \mathbf{g}_M(\omega)] \quad (13)$$

Hence, the received vector  $\mathbf{y}(\omega) = [y_1(\omega), \dots, y_M(\omega)]^T$  is

$$\mathbf{y}(\omega) = \mathbf{H}(\omega)\mathbf{G}(\omega)\mathbf{x}(\omega) + \mathbf{w}(\omega) \quad (14)$$

where  $\mathbf{w}(\omega)$  is the noise vector with a complex Gaussian distribution. Let  $x_m(\omega)$  be the information bearing signal intended for the  $m$ -th user, and  $\mathbf{x}(\omega) = [x_1(\omega), \dots, x_M(\omega)]$  be the transmitted data vector. For simplicity, we assume that  $E\{\mathbf{x}(\omega)\mathbf{x}^H(\omega)\} = \sigma_x^2\mathbf{I}$ . We further adopt a discrete signal model where the channel is sampled at discrete frequency values  $\omega_q$ . We assume that  $Q = \frac{\text{BW}}{B_c} > 1$  is the total number of frequency samples and  $B_c$  is the correlation bandwidth of the propagation medium and is the inverse of the maximum differential delay spread due to multipath. BW is the bandwidth of the information signals. Note that frequency samples collected one correlation bandwidth apart are approximately independent and denser multipath implies a smaller  $B_c$ . Thus, we can consider  $\mathbf{H}(\omega_q)$  at different  $\omega_q$  as independent channels [13]. Such a treatment will facilitate our development when  $Q \rightarrow \infty$ . We drop the argument  $\omega_q$  for the moment. Plugging (11) and (12) into (14) yields

$$\begin{aligned} \mathbf{y}(\omega) &= \mathbf{H}(\omega) [\mathbf{H}^H(\omega)\mathbf{H}(\omega)]^{-1} \mathbf{H}^H(\omega)\mathbf{\Pi}\mathbf{x}(\omega) + \mathbf{w}(\omega) \\ &= \mathbf{P}_{\mathbf{H}(\omega)}\mathbf{\Pi}\mathbf{x}(\omega) + \mathbf{w}(\omega) \end{aligned} \quad (15)$$

where

$$\mathbf{\Pi} = \text{diag}[\eta_1, \dots, \eta_M] \quad (16)$$

$\mathbf{P}_{\mathbf{A}} = \mathbf{A}(\mathbf{A}^H\mathbf{A})^{-1}\mathbf{A}^H$  is the orthogonal projection onto the  $\min(M, N)$  dimensional subspace  $\langle \mathbf{A} \rangle$ . Let  $\mathbf{H}(\omega) = \mathbf{U}(\omega)\mathbf{\Gamma}(\omega)\mathbf{V}^H(\omega)$  be the singular value decomposition; we obtain

$$\mathbf{P}_{\mathbf{H}(\omega)} = \mathbf{U}(\omega)\mathbf{\Lambda}(\omega)\mathbf{U}^H(\omega) \quad (17)$$

where the diagonal matrix  $\mathbf{\Lambda}(\omega) = \text{diag}[\underbrace{1, \dots, 1}_l, \underbrace{0, \dots, 0}_{\min(M, N) - l}]$  and  $l$  is the rank of  $\mathbf{H}(\omega)$ .

For full rank matrix,  $\mathbf{\Lambda} = \mathbf{I}$  and  $\mathbf{P}_{\mathbf{H}(\omega)} = \mathbf{I}$ .

The proposed beamformer (11) resembles the zero-forcing beamformer (see, e.g., [14, 15]) at frequency  $\omega$ . However, the two schemes are different. If two mobile users sharing the same channel are close to each other, the channel matrix  $\mathbf{H}(\omega)$  will become singular. This implies that there will be cross talk between the two users. Therefore, the narrowband zero-forcing beamforming is not designed for singular

channels. Consequently, the base station should assign one receiver to a new channel. However, this strategy is not appropriate in ultra-wide band systems.

The proposed time reversal beamformer utilizes multipath in wideband to overcome this problem. Due to multipath propagation, the channel spectrum for each user will change significantly over the operating frequency range. The channel spectrum will appear to be random. As a result, the channel matrix  $\mathbf{H}(\omega)$  may not be singular at  $\omega$  even if it is singular at  $\omega'$ . Therefore, the cross talk can be reduced and the system capacity can be improved. Given (15), the maximum achievable data rate (capacity) for user  $m$  is [16]

$$R_m^{\text{TRBF}}(\omega) = \log_2 \left( 1 + \frac{\sigma_x^2 |\eta_m|^2}{\sigma_w^2} \right). \quad (18)$$

Noticing that  $R_m^{\text{TRBF}}(\omega)$  is Riemann integrable on the interval  $[-\pi, \pi]$ , we obtain the total capacity [17]

$$R_m^{\text{TRBF}} = \frac{1}{2\pi} \int_{-\pi}^{\pi} R_m^{\text{TRBF}}(\omega) d\omega = \log_2 \left( 1 + \frac{\sigma_x^2 |\eta_m|^2}{\sigma_w^2} \right). \quad (19)$$

Hence, the sum rate capacity  $R$  is given by

$$R = \max \sum_{m=1}^M R_m^{\text{TRBF}} = \max \sum_{m=1}^M \log_2 \left( 1 + \frac{\sigma_x^2 |\eta_m|^2}{\sigma_w^2} \right). \quad (20)$$

What remains to be calculated is the  $\{\eta_m\}$  subject to the transmit power constraint

$$\int \text{tr}\{\mathbf{G}(\omega)\mathbf{G}^H(\omega)\}d\omega \leq P_M, \quad (21)$$

where  $P_M$  is the total transmission power. Hence, the elements  $\{\eta_m\}$  are selected by

$$[\eta_1, \dots, \eta_M] = \arg \max_{\int \text{tr}\{\mathbf{G}(\omega)\mathbf{G}^H(\omega)\}d\omega \leq P_M} \sum_{m=1}^M R_m^{\text{TRBF}}. \quad (22)$$

The optimal solution of (22) is the water-filling algorithm. In fact, let  $\Phi(\omega) = \mathbf{U}(\omega)\Gamma^{-2}(\omega)\mathbf{U}^H(\omega)$ , then

$$\begin{aligned} \int \text{tr}\{\mathbf{G}(\omega)\mathbf{G}^H(\omega)\}d\omega &= \int \text{tr}\{\Phi(\omega)\Pi^2\}d\omega \\ &= \sum_{m=1}^M \phi_{mm} \eta_m^2 \end{aligned} \quad (23)$$

where  $\phi_{ii} = \int [\Phi(\omega)]_{ii} d\omega$ , and  $[\mathbf{A}]_{ii}$  is the  $i$ -th diagonal component of matrix  $\mathbf{A}$ . Hence, employing the water-filling approach [16], we have

$$\hat{\eta}_m = \sqrt{\frac{1}{\phi_{mm}} \left( v - \frac{\sigma_w^2}{\sigma_x^2} \right)^+} \quad (24)$$

where  $(x)^+$  denotes the positive part of  $x$  and  $v$  is the chosen water-line so that

$$\sum_m \phi_{mm} \left( v - \frac{\sigma_w^2}{\sigma_x^2} \right)^+ = P_M \quad (25)$$

As a result, the focusing gain is chosen to be

$$\gamma_m = \hat{\eta}_m \int \mathbf{c}_m^T(\omega)(\mathbf{H}^H(\omega)\mathbf{H}(\omega))^{-1}\mathbf{c}_m^*(\omega)d\omega \quad (26)$$

**Dirty Paper Coding:** Dirty paper coding (DPC) is the capacity achieving strategy in MIMO broadcasting channels. DPC was originally developed by Costa [8] on known-interference cancellation at the transmitter. The result shows that, when encoding the desired user's signal, the transmitter can perform a pre-cancellation of the interfering signal without a power or rate penalty, a process termed "writing on dirty paper." In the context of a multiuser Gaussian broadcast channel, the DPC coding technique ensures that the given user will not suffer any interference from all the previously encoded users.

Before implementing the DPC coding, we wish to design the filter  $\mathbf{G}(\omega)$  such that the overall filter response  $\mathbf{H}(\omega)\mathbf{G}(\omega)$  in (14) becomes a lower triangular matrix that permits application of the DPC. We can choose

$$\mathbf{G}^{\text{DPC}}(\omega) = \mathbf{Q}(\omega)\mathbf{\Psi}(\omega) \quad (27)$$

(see also [9]) where  $\mathbf{\Psi}(\omega)$  is a diagonal power matrix and  $\mathbf{Q}(\omega)$  is obtained from the  $QR$  decomposition of the matrix  $\mathbf{H}^H(\omega) = \mathbf{Q}(\omega)\mathbf{R}(\omega)$ , where  $\mathbf{R}(\omega)$  is an upper diagonal matrix. Hence, (14) becomes

$$\mathbf{y}(\omega) = \mathbf{R}^H(\omega)\mathbf{\Psi}(\omega)\mathbf{x}(\omega) + \mathbf{w}(\omega). \quad (28)$$

Let  $[\mathbf{G}^{\text{DPC}}(\omega)]_{ij} = g_{ij}(\omega)$ ; we obtain

$$y_m(\omega) = g_{mm}(\omega)x_m(\omega) + \sum_{i=1}^{m-1} g_{mi}(\omega)x_i(\omega) + w_m(\omega). \quad (29)$$

The achievable rate for user  $m$  by the DPC coding scheme is given as follows: (Due to space limitation, we omit the details of the DPC implementation.)

$$R_m^{\text{DPC}} = \frac{1}{2\pi} \int_{-\pi}^{\pi} \log_2 \left( 1 + \frac{\sigma_x^2 |g_{mm}(\omega)|^2}{\sigma_w^2} \right) d\omega \quad (30)$$

where the diagonal entry  $g_{mm}(\omega) = [\mathbf{R}^H(\omega)]_{mm}[\mathbf{\Psi}(\omega)]_{mm}$ .  $\mathbf{\Psi}(\omega)$  is chosen subject to the power constraint (21).

$$\begin{aligned} \int \text{tr}\{\mathbf{G}^{\text{DPC}}(\omega)\mathbf{G}^{\text{DPC},H}(\omega)\}d\omega &= \int \text{tr}\{\mathbf{\Psi}^2(\omega)\}d\omega \\ &= \sum_{i=1}^M \int |\psi_{ii}(\omega)|^2 d\omega \leq P_M \end{aligned}$$

where  $\psi_{ii}(\omega) = [\Psi(\omega)]_{ii}$  and can be found from the space-frequency water-filling solution

$$\hat{\psi}_{mm}(\omega) = \sqrt{\left(v - \frac{\sigma_w^2}{\sigma_x^2 |r_{mm}(\omega)|^2}\right)^+} \quad (31)$$

The sum rate capacity is

$$R^{\text{DPC}} = \max \sum_m R_m^{\text{DPC}} = \sum_m R_m^{\text{DPC}}(\hat{\psi}_m) \quad (32)$$

**Equal Power Transmission:** The equal power transmission (EPT) scheme assigns each user to a dedicated antenna with equal transmission power and no pre-filtering. In this case,  $\mathbf{G}^{\text{EPT}}(\omega) = \sqrt{\frac{P_M}{M}} \mathbf{I}$ . Thus, the achievable data rate is given by

$$R_m^{\text{EPT}} = \frac{1}{2\pi} \int_{-\pi}^{\pi} \log_2 \left( 1 + \frac{\sigma_x^2 |c_{mm}(\omega)|^2 \frac{P_M}{M}}{\sigma_x^2 \sum_{i \neq m} |c_{mi}(\omega)|^2 \frac{P_M}{M} + \sigma_w^2} \right) d\omega \quad (33)$$

The sum rate capacity is  $R^{\text{EPT}} = \sum_m R_m^{\text{EPT}}$ .

## 4 FDTD Scattering Channel Simulations

We use the finite-difference time-domain (FDTD) method to simulate the propagation channels in a rich scattering environment. The scattering environment contains 24 scatterers placed randomly in a region shown in Fig. 2. Energy arrives at the receivers only via local scatterers, and no light of sight is present. Users are placed in a region of  $[25\lambda_c \ 45\lambda_c] \times [-10\lambda_c \ 10\lambda_c]$ . The FDTD modeling grid cell size is chosen to be  $0.5 \times 0.5 \text{ mm}^2$ . The resulting FDTD grid is terminated with the Perfect Matched Layer (PML) absorbing boundary condition. The probing signal is a sinc signal of 2 GHz bandwidth with the center frequency of 5 GHz. The wavelength is  $\lambda_c = 6 \text{ cm}$ . We choose  $Q = 201$  frequency sample points from 4 – 6 GHz bandwidth. The FDTD simulated data are time domain samples, and can be converted to frequency domain via the Fourier transform.

## 5 Numerical Results

Numerical studies are carried out to evaluate the performance of an adaptive array sharing a frequency band among 3 user terminals simultaneously. We use a linear array of 3 antennas with inter-element spacing of  $2\lambda_c$ . We define SNR as  $10\log_{10}(\sigma_x^2/\sigma_w^2)$ .

Fig. 3 depicts the SINR of an intended user sharing a channel with other two users versus user spacing in wavelength. We fix the intended user and let two other users approach him from two sides symmetrically. We calculate the SINR of the TRBF under the rich scattering condition and no scattering condition, respectively. Under no scattering condition, the scatterers are removed in the FDTD simulation. The left figure shows the SINR plot when the two

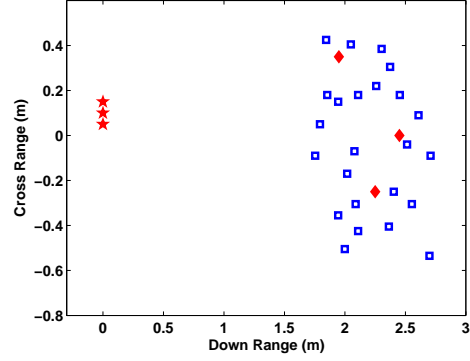


**Figure 2. A multiuser simulation scenario. The pentagram denotes the antennas, the squares denote the scatterers, and the diamonds indicate possible user locations.**

users approach the intended user along the down range. The right figure is for the cross range scenario. In both cases, the TRBF under the rich scattering condition yields higher SINR compared with the no scattering condition. In particular, the large gain (about 6 dB) shown in the left figure demonstrates that rich scattering is very helpful in down range signal detection for users at the same azimuth.

Fig. 4 depicts the sum rate capacity of the TRBF as the SNR changes under the conditions of no scattering (upper figure) and rich scattering (lower figure). The results show that, with a rich scattering, the TRBF provides higher gain when compared with the equal power transmission scheme. For example, at SNR = 10 dB, the averaged user rate gain between TRBF and the EPT method is about 2.2 bits/symbol with rich scattering. This gain is reduced to 0.3 bits/symbol with no scattering. Furthermore, the TRBF has a performance closer to the DPC coding scheme under a rich scattering condition.

## 6 Conclusion

We have proposed the time reversal wideband beamformer that exploits dense multipath environment to achieve low signal crosstalk at intended users terminals. Simulations show that dense scattering can be used to advantage to improve system performance.

## References

- [1] Y. Jin, Y. Jiang, and J. M. F. Moura, "Multiple antenna time reversal transmission in ultra-wideband communications," in *Proceedings of IEEE Globecom*. IEEE, November 2007.

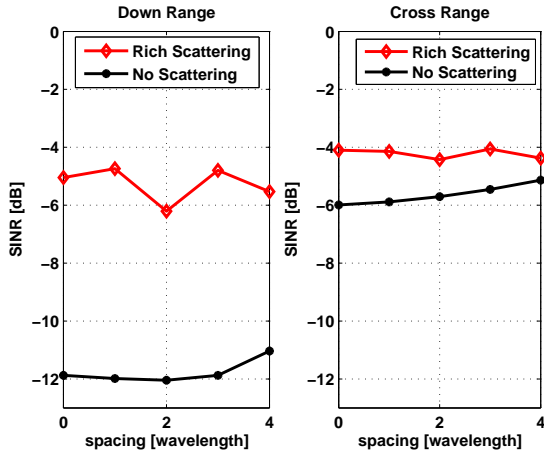


**Figure 3. SINR vs. user spacing in wavelength. A fixed user is approached by two other users. Left figure - down range; Right figure - cross range.**

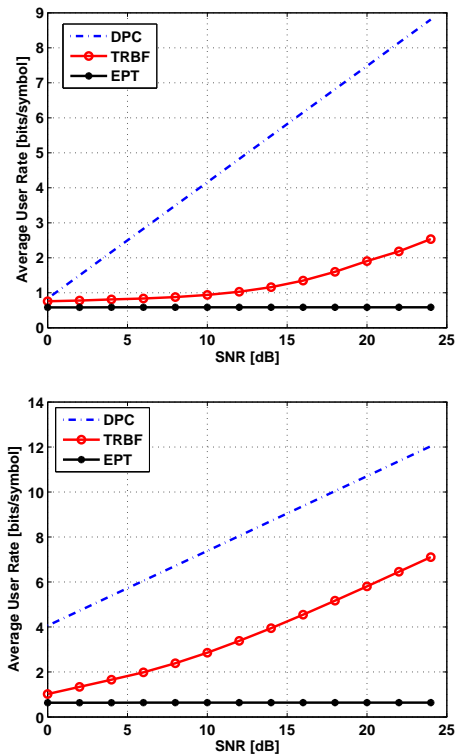


**Figure 4. Average data rate in bits per symbol versus SNR for TR beamformer, equal power transmission scheme, and the DPC coding. Upper figure - no scattering; Lower figure - rich scattering**

- [2] J. M. F. Moura and Y. Jin, "Detection by time reversal: single antenna," *IEEE Transactions on Signal Processing*, vol. 51, no. 1, pp. 187–201, January 2007.
- [3] P. Blomgren, P. Kyritsi, A. D. Kim, and G. Papanicolaou, "Spatial focusing and intersymbol interference in multiple-input/single-output time reversal communication systems," *IEEE Journal of Oceanic Engineering*.
- [4] A. J. Paulraj and C. B. Papadias, "Space-time processing for wireless communications," *IEEE Signal Processing Magazine*, vol. 14, pp. 49–83, November 1997.
- [5] J. Xavier, V. A. Barroso, and J. M. F. Moura, "Closed-form blind channel identification and source separation in SDMA systems through correlative coding," *IEEE Journal on Selected Areas in Communications*, vol. 16, no. 8, pp. 1506–1517, October 1998.
- [6] M. Joham, W. Utschick, and J. A. Nossek, "Linear transmit processing in MIMO communications systems," *IEEE Transactions on Signal Processing*, vol. 53, no. 8, pp. 2700–2712, August 2005.
- [7] D. D. Stancil, A. G. Cepni, B. E. Henty, Y. Jiang, Y. Jin, J.-G. Zhu, and J. M. F. Moura, "Super-resolution focusing and nulling in rich multipath environments using time-reversal techniques," in *International Conference on Electromagnetics in Advanced Applications (ICEAA)*. IEEE, April 2005.
- [8] M. Costa, "Writing on dirty paper," *IEEE Transactions on Information Theory*, vol. 29, pp. 439–441, May 1983.
- [9] D. Samardzija, N. Mandayam, and D. Chizhik, "Active transmitter optimization in multiuser multi-antenna systems: theoretical limits, effect of delays and performance enhancements," *EURASIP Journal on Wireless Communications and Networking*, no. 3, pp. 298–307, August 2005.
- [10] L. Smolyar, I. Bergel, and H. Messer, "Multi-user sum-rate capacity for ultra-wideband radio," *IEEE Transactions on Wireless Communications*, vol. 5, no. 7, pp. 1818–1826, July 2006.
- [11] A. Cepni, "Experimental investigation of time reversal techniques using electromagnetic waves," Ph.D. dissertation, Carnegie Mellon University, 2005.
- [12] G. B. Arfken and H. J. Weber, *Mathematical Methods for Physicists*. Burlington, MA: Elsevier Academic Press, 2005.

- [13] A. J. Goldsmith and M. Effros, "The capacity region of broadcast channels with intersymbol interference and colored gaussian noise," *IEEE Transactions on Information Theory*, vol. 47, no. 1, pp. 219–240, January 2001.
- [14] H. Viswanathan, S. Venkatesan, and H. Huang, "Downlink capacity evaluation of cellular networks with known-interference cancellation," *IEEE Journal on Selected Areas in Communications*, vol. 21, no. 5, pp. 802–811, June 2003.
- [15] T. Yoo and A. Goldsmith, "On the optimality of multiantenna broadcast scheduling using zero-forcing beamforming," *IEEE Journal on Selected Areas in Communications*, vol. 24, no. 3, pp. 528–541, March 2006.
- [16] T. M. Cover and J. A. Thomas, *Elements of Information Theory*. New York, NY: John Wiley & Sons, 1973.
- [17] W. Rudin, *Principles of Mathematical Analysis*. New York, NY: McGraw Hill, 1973.